

## COLLECTION OF PETROLEUM CRUDE OIL SPILL POLLUTANTS FROM SEA WATER USING HIGH MAGNETIZATION ANTIMICROBIAL BIOCOMPATIBLE MAGNETITE NANOPARTICLES

A. M. ATTA<sup>a,b\*</sup>, H. A. AL-LOHEDAN<sup>a</sup>, S. A. AL-HUSSAIN<sup>a,c</sup>

<sup>a</sup>*Surfactants research chair, Department of Chemistry, College of Science, King Saud University, Riyadh 11541, Kingdom of Saudi Arabia.*

<sup>b</sup>*Egyptian Petroleum Research Institute, 1 Ahmad Elzomor St., Nasr city 11727, Cairo, Egypt.*

<sup>c</sup>*Chemistry department, faculty of science, Al- Imam Muhammad Ibn Saud Islamic University, Riyadh 11632, Kingdom of Saudi Arabia.*

This work aims to synthesize mass production of uniform magnetite nanoparticles (up to 50 g) with a core sizes between 10 and 20 nm for environmental application. Fatty acids such as stearic, oleic and linoleic and linolenic acids were used as capping agents. The chemical structure of magnetite nanoparticles capped with fatty acids crystal sizes and morphologies revealed that magnetite nanoparticles were encapsulated into the shells of fatty acids. The magnetic properties and antimicrobial activities of the prepared magnetite nanoparticles confirmed the application of nanoparticles for environmental application as crude oil collector for oil spill using an external magnetic field.

(Received January 7, 2016; Accepted February 26, 2016)

**Keyword:** Magnetite; Fatty acids; Magnetic properties; Oil spill collector; Nano-cube; Antimicrobial

### 1. Introduction

The inorganic nanomaterials attracted great attention to be the core of future developments in industrial and technological applications [1]. Iron oxide magnetic NPs (MNPs) have many advantages and are considered very promising nanomaterials that can be handled by using an external magnetic field. MNPs amongst materials with magnetic properties, due to their proven biocompatibility, are most suitable for biomedical and environmental applications [1-3]. The use of advanced nanotechnology in water purification for the production of safe drinking water is currently investigated. The most common iron oxide nanoparticles; magnetite and maghemite exhibit unique physical and chemical particularities [4]. Magnetic iron oxide nanoparticles ( $\text{Fe}_3\text{O}_4$ ) are common ferrite exhibit unique magnetic properties due to the electrons transfer between  $\text{Fe}^{2+}$  and  $\text{Fe}^{3+}$  in the octahedral sites which has a cubic inverse spinel structure. However, Food and Drug Administration approved the clinical use of magnetite and maghemite because of their inherent properties and biocompatibility as they naturally occurred in the human heart, spleen and liver. These materials showed antimicrobial activity when they interacted with microbial cells as small size to destroy the microbial cell without poisoning of human body (5, 6). In recent years, scientists valorized the potential of magnetite nanoparticles in the inhibition of microbial growth and bio-film formation of many pathogenic species, such as fungi, yeasts and bacteria this besides treating specific infectious diseases [7-10]. It was also reported that magnetite nanosystems exhibited antimicrobial activity against planktonic, as well as adherent microbial cells [11].

Preparation of  $\text{Fe}_3\text{O}_4$  nanoparticles has attracted great interest because of their immense usefulness in different domains, especially in the form of ferro-fluids at size scales of less than 100 nm because of their high reactivity due to the large surface-to-volume ratio [12-13]. There are

---

\* Corresponding author: aatta@ksu.edu.sa

many limitations arise from preparation of magnetite such as particle agglomerations, dispersability and stability in aqueous system. Different types of stabilizing agents were introduced to control the stability of magnetic nanoparticles however most of these materials leads to increased cytotoxicity. New strategies were used to improve the antimicrobial activity of MNPs using oils, plants extracts, titania and microwave exposure [14-18]. Many researches aim to use different synthetic routes to prepare magnetite nanospheres, nanocubes, nanoneedles and nanoporous using hydrothermal methods [19], co-precipitation methods [20], solvo-thermal methods [21, 22], sonochemical methods [23] and self-assembly methods [19]. The magnetic, electrical and optical properties of magnetite strongly depend on their dimension, shape, saturation magnetization as well as monodispersability [23, 24]. The limitation of co-precipitation method to spherical shape limits the properties and applicability of the prepared particles. Different preparation techniques rather than coprecipitation such as solvo-thermal [23], hydrothermal [25], and template [26] methods, have been widely used to synthesize magnetic nanomaterials having different morphologies (nanocubes, nanoplates, nano-needles or nanorods). These methods are expensive and have low yield. In the present work, it is the first time to prepare different shapes of coated magnetite nanoparticles rather than spherical nanoparticles. One of the objectives of this study is to synthesize iron oxide magnetic nanoparticles (magnetite) by simple chemical co-precipitation method using one iron salt at room temperature. Moreover, the production of high yield and different shapes of biocompatible magnetite coated nanoparticles is another objective of this work. The evaluation of antibacterial activity after treating with different types of fatty acids is not so far reported in the earlier literature. So, extensive study is conducted to examine the antibacterial activity of magnetic nanoparticles. The application of the prepared magnetite nanoparticles to collect the petroleum crude oil spill using magnetic field is investigated.

## **2. Experimental**

### **2.1 Materials**

Anhydrous ferric chloride, potassium iodide and aqueous (25%) ammonium hydroxide solution used as reagents for preparation of magnetite were purchased from Aldrich Chemical Co. (St. Louis, MO, USA). Oleic acid (OA), stearic acid (SA), linoleic acid (LOA) and linolenic acid (LNA), were obtained from Sigma Chemicals (St. Louis, MO, USA). The Arabian heavy crude oil produced by ARAMCO, Ras Tanora oil field was used as source of oil spill.

### **2.2. Preparation Technique**

The capped magnetite nanoparticles with fatty acid can be prepared by reacting a solution of anhydrous  $\text{FeCl}_3$  (40 g; in 300 mL of water ) with KI (13.2 g, in 50 water) at room temperature. The reaction mixture was stirred for one hour until iodine was precipitated. Different amounts of SA, OA, LOA or LNA solubilized in ethanol-water solvent (100 mL, 4:1 vol%) and 25% ammonia solution (200 mL) were added dropwise at the time to the heated reaction mixture at 55 °C. The reaction mixture kept at this temperature for 4 h until complete precipitation of black magnetite was achieved. The precipitate was then left to settle down, filtered, washed with distilled water, ethanol, dried under vacuum at 30 °C and weighed. The percentage yields were 99.1%, 90.3, 92.5 and and 95.5% for magnetite coated with SA, OA, LOA and LNA, respectively.

### **2.3 Characterization**

Fourier transform infrared (FTIR) spectroscopic analysis of the samples was performed using a Spectrum One FTIR spectrometer (Perkin-Bhaskar-Elmer Co., USA).

The crystal structure of magnetite capped with fatty acids were characterized on x-ray powder diffraction (XRD; BDX-3300 diffractometer using  $\text{CuK}\alpha$  radiation wavelength,  $\lambda=1.5406\text{\AA}$ ).

The morphologies of magnetite capped with fatty acids were determined using high-resolution transmission electron microscopy (HR-TEM; JEM-2100 F; JEOL, Japan).

The particle size distribution of magnetite capped with fatty acids was determined from dynamic light scattering (DLS; Zetasizer Nano ZS; Malvern Instruments, Malvern, U.K.) with a

633 nm He-Ne laser using ethanol/water (4/1) as solvent. The nanoparticles size was further measured by DLS at 25 °C. Zeta potentials of magnetite and nanogel suspensions were measured at 25 °C using a zeta potential analyser. Particle suspensions were diluted with deionized water or 0.001 mol L<sup>-1</sup> KCl prior to measurements.

Thermal stability and magnetite contents of magnetite capped with fatty acids were investigated using thermogravimetric analysis (TGA; Shimadzu, DTG-60M) at a heating rate of 10 °C min<sup>-1</sup>.

Size distribution and zeta potential of the magnetic nanogel were determined by a Zetasizer 3000HS PCS (Malvern Instruments).

Surface tension measurements of the dispersed magnetite in water were carried out at different molar concentrations and at temperature 45 °C by means of the pendant drop technique using a drop shape analyser (model DSA-100, Kruss, Germany).

The magnetic measurement of the products was carried out in a USALDJ9600-1 vibrating sample magnetometer (VSM). Magnetic hysteresis loops were recorded at room temperature in a field of 20,000 Oe to determine the saturation magnetization (Ms) for the samples.

#### **2.4 Antimicrobial properties of samples**

The antimicrobial activities of magnetite capped with fatty acids included minimum inhibitory concentration (MIC) and minimum bactericidal concentration (MBC) of the samples were determined using the broth-micro dilution test against three common strains of bacteria; *Escherichia coli* ATCC 8739, *Staphylococcus aureus* ATCC 6538, *Bacillus subtilis* ATCC 6633 and *Pseudomonas aeruginosa* ATCC 10145 as reported in our previous work [27].

#### **2.5 Evaluation of the magnetite nanoparticles as oil collector:**

The removal efficiency of magnetic powder toward oil spill was evaluated according previous reported method [27] by comparing the volume of oil removed using this clean-up procedure to the volume of the original oil spill and quantified in a variable called "efficiency" which can be calculated as; Efficiency = (volume of removed oil/ volume of original spill) \* 100%. The magnetite powders were separated from removed oil and reused three times.

### **3. Results and discussion**

The stability of iron oxide nanoparticles in solution is one of utmost challenges for its applications and storage process. The interactions between the iron oxide particles increased particle size due to strong magnetic dipole-dipole attractions between the agglomerated particles. Accordingly, surface modification of magnetic nanoparticles is often necessary to mitigate magnetic interaction. It is necessary to modify the surface of the nanoparticles with substances that make them stable in the dispersion medium. In this respect, stabilization of preformed iron oxide nanoparticles can be achieved via either electrostatic or steric stabilization. The present work deals with the preparation of iron oxide with cheap method and coating with fatty acid to apply as petroleum crude oil collector by external magnetic field. The evaluation of the antimicrobial activity of the prepared iron oxide is another goal of the present work. The strategy of work is based on capping the iron oxide nanoparticles with bio-materials to increase the particle dispersability without increasing the particle size more than 20 nm to control the magnetic properties of the prepared iron oxide nanoparticles. The stabilization of iron oxide nanoparticles is achieved by adsorption of fatty acid during the formation of the nanoparticle surface. Stearic (SA), oleic (OA), linoleic (LOA) and linolenic (LNA) acids were used as capping agent to assemble a monolayer of these molecules on the nanoparticle surface produces oil- based magnetic fluid. The aqueous-based magnetic fluid can be produced by assemblies of bilayers of these molecules. It was expected that the unsaturated fatty acid such as LNA, LOA, OA can form a dense protecting monolayer on the particle than SA where the double bond provides a kink necessary for such a small molecule to provide effective stabilization.

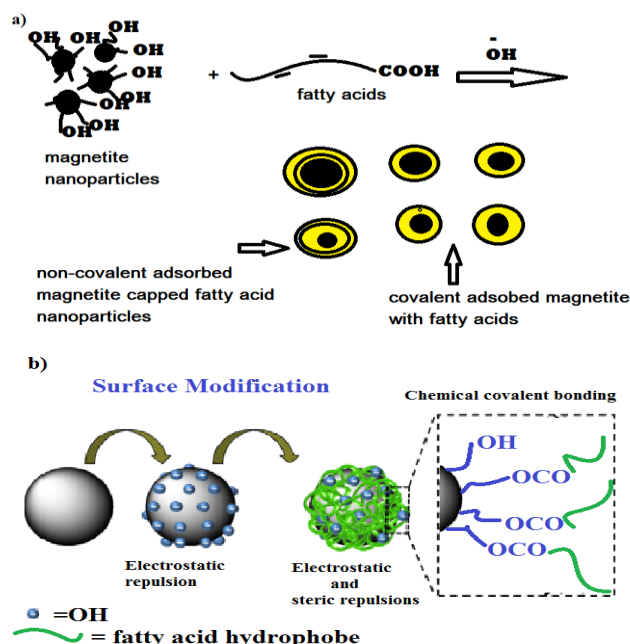
### 3.1. Capping of magnetite with fatty acids

In the previous [27-32], we succeeded to prepare magnetite and iron oxide nanoparticles using simple method which only requires one iron salt as starting precursor, a limited number of additional chemical reagents, and low process temperature lower than 50 °C.

The production of magnetite nanoparticles can be carried out according to the following equations:



The first reaction depends on formation of ferrous and ferric ions and iodine. The iron oxides can be produced after removal of iodine followed by precipitation in basic medium [33]. In the previous work [31, 32] iodine was not removed and forms hypoiodite ( $\text{IO}^-$ ) and iodate ( $\text{IO}_3^-$ ) in basic medium anions as suggested in equations 2 and 3. The equilibrium of this reaction can move to either side, depending on the pH of the solution. It was reported that the adsorption of iodate anion on iron oxide influenced the crystal growth of magnetite and produce more hydroxyl groups [31, 32, and 34]. The formation of hydroxyl groups on the surface of iron oxide nanoparticles can enhance the capping of the particles with fatty acid and these groups are able to form covalent bonds with carboxylic functional groups of fatty acids to avoid their agglomeration. Thus, stabilization may be attributed to formation of a passivation layer and/or to electrostatic repulsion. The stabilization scheme can be illustrated by Scheme 1.



Scheme 1: Synthesis of magnetite capped fatty acid particles.

The concentrations of fatty acids play an important role in capping of magnetite. It is well known that when the concentration of fatty acids exceeds the critical micelle concentration, micelle formation will occur. This will reduce the amount of fatty acids available for particles stabilization. SA, OA, LOA and LNA were separated from preparation solution as blank without iron oxide at the same time and temperature of the reaction medium. The critical micelle concentrations (CMC) determined using drop shape analyzer (DSA-100) from variation of surface tension and  $-\ln c$  where  $c$  is the concentrations of fatty acids. The CMC values were determined at 45 °C are 0.08, 3.3, 6.8 and 9.1 mM for SA, OA, LOA and LNA, respectively. The CMC values

were increased with increasing the number of double bond in fatty acids [35]. These concentrations were used to prepare capped magnetite nanoparticles to prevent micelle formation by adding fatty acid in portions. It was expected that the stabilization of magnetite nanoparticles with fatty acids at high pH is attributed to absorption of hydroxide [27] ions at the particle surface and subsequent charge stabilization of the magnetic particles. It is envisaged that at high pH, OH<sup>-</sup> ions are absorbed onto that part of the surface of the particle not occupied by carboxylic groups of fatty acids. Increasing the reaction temperature up to 45-55 °C is necessary to maintain Fe<sub>3</sub>O<sub>4</sub> nanoparticles in a dispersed state during addition of fatty acids.

### 3.2. Characterization of the prepared nanoparticles

FTIR spectra of iron oxide particles prepared in the presence and absence of iodine are presented in Fig.1a and b, respectively. The spectra indicate the presence of magnetite from appearance of characteristic absorption band of Fe-O at band at 570 cm<sup>-1</sup> (Fig. 1).

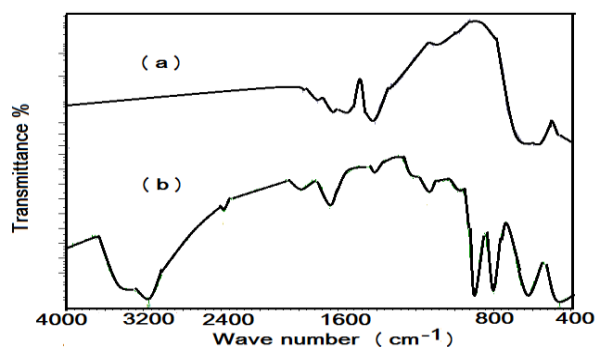


Fig.1: FTIR spectra of magnetite nanoparticles prepared with a) removal of iodine and b) the presence of iodine.

Fig.1b shows new bands at 650 and 750 cm<sup>-1</sup> indicating the presence of maghemite [32]. Moreover, the spectrum in Fig.1b indicates the presence of  $\alpha$ -Fe<sub>2</sub>O<sub>3</sub> (hematite) nanoparticles, revealed by a large and intense band at 3450 cm<sup>-1</sup> that could be assigned to the structural OH groups. The capping of magnetite with fatty acids was confirmed by FTIR analysis. Moreover the type of capping through physical or chemical adsorptions was confirmed by FTIR. In this respect, FTIR spectra of magnetite nanoparticles capped with SA or LNA were selected as representative samples and represented in Fig. 2 a and b.

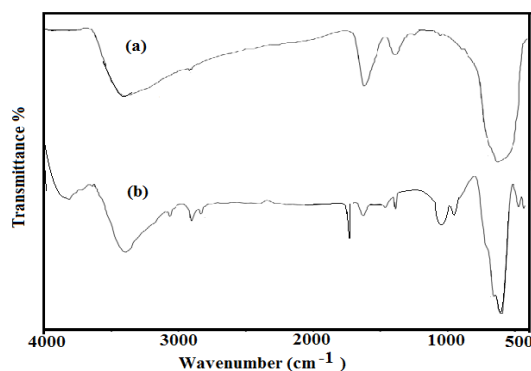


Fig.2: FTIR spectra of magnetite nanoparticles capped with a) SA and b) OA.

All spectra of the nanoparticles show absorption bands at 2922 and 2852 cm<sup>-1</sup> which attribute to shifted bands of the asymmetric and symmetric CH<sub>2</sub> stretch. All spectra of magnetite

coated with OA, LOA and LNA showed absorption bands Fe-O stretching of magnetite at 578 and 628  $\text{cm}^{-1}$ . The bands at 1740 and 1090  $\text{cm}^{-1}$  (C=O and -C-O stretching, respectively) observed in spectra of magnetite coated with OA, LOA and LNA whereas these bands disappeared in the spectrum) of magnetite coated with SA. These bands indicate the formation of ester group at magnetite surfaces in the presence of unsaturated fatty acids. The absence of ester bond between SA and magnetite attributed to the attraction between alkyl groups of SA at magnetite surface which hinders the chemisorption at magnetite surfaces. It is also observed that the strong band at 3424  $\text{cm}^{-1}$  attributed to the symmetric O-H stretching vibration of hydroxyl groups that are absorbed onto that part of the surface of the particle not occupied by surfactant groups as well as  $\nu(\text{O-H})$  for H-bonded OH groups (from OA). FTIR spectrum of SA coated  $\text{Fe}_3\text{O}_4$  nanoparticles (Fig. 2 a) clearly reveals the presence of strong band at 580  $\text{cm}^{-1}$  that is belong to Fe-O stretching, while bands at 3424  $\text{cm}^{-1}$  and 2921  $\text{cm}^{-1}$  attributed to the COOH group of stearic acid and C-H stretching of the hydrocarbon chain. FTIR spectra indicate disappearance of absorption bands of maghemite at 750  $\text{cm}^{-1}$  with attributed to capping of particles which decrease the possibility of oxidation and conversion of magnetite to maghemite.

The quantity of fatty acid SA, OA, LOA and LNA capped magnetite after removal the uncapped fatty acid by ethanol washing can be determined from TGA. In this respect, TGA thermograms were represented in Fig. 3.

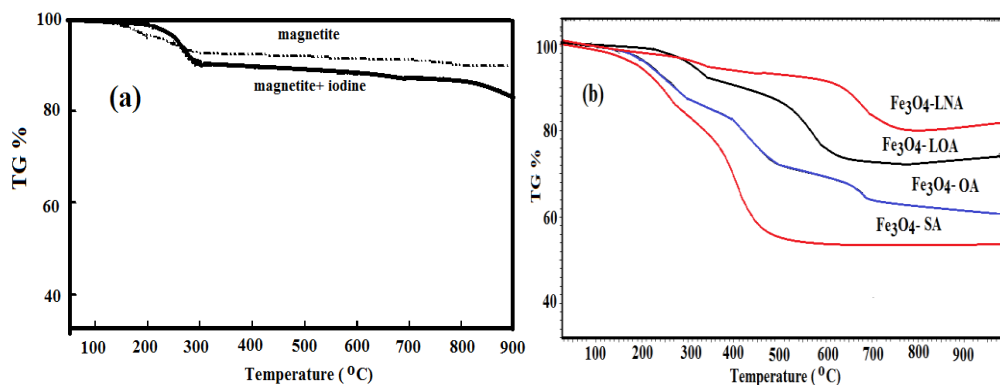


Fig.3. Thermograms of a) magnetite and b) capped magnetite nanoparticles.

The thermograms of uncapped magnetite prepared in the presence and absence of iodine (Fig.3 a) indicates that magnetite losses 10.23 and 16.8 % ( w/w) respectively up to 270 °C for that prepared in absence and presence of iodine, respectively which referred to water decomposition arises from hydroxyl groups at magnetite surfaces. Interesting is the suppression in the magnetite nanoparticles of the unexpected weight gain in the 120-210°C temperature range, attributable to the oxidation of magnetite to maghemite [36, 37]. Moreover, thermograms of magnetite coated with fatty acids (Fig. 3b and c) confirm the a rapid weight loss between 160 and 300°C due to the thermal decomposition of the fatty acids. The data indicates that the magnetite coated with fatty acids in the presence of iodine contain more magnetite than that coated in absence of iodine. This can be attributed to the possibility to form covalent bonds between hydroxyl groups of magnetite surfaces in the presence of iodine is more than that occurred in absence of iodine (scheme 1). Furthermore, the increment of double bond contents in fatty acids decreases the contents of fatty acids capped magnetite and this refers to steric hindrance repulsion force as described in scheme 1. The data indicated that the magnetite contents of magnetite capped with SA, OA, LOA and LNA in the presence of iodine are 56.2, 62.3, 73.4 and 78.2 %, respectively. While the magnetite contents for that prepared in the absence of iodine are 57.3, 63.4, 68.2 and 72.4, respectively. These data indicate that the fatty acid coating molecules also limit the reactivity of the MNCs surface to oxidation to maghemite with the environment in comparison to other uncoated nanoparticles.

XRD is useful technique to determine the purity of the prepared magnetite and also used to study the effect of coating on the magnetite crystal shapes. In this respect XRD diffractograms of

iron oxide prepared in the presence of iodine and fatty acid as capping agents are represented in Fig. 4 a-d. In the previous work, the XRD indicated that pure magnetite nanoparticles were prepared by removal of iodine from the reaction medium [32]. While both  $\alpha$  and  $\gamma$  phases of  $\text{Fe}_2\text{O}_3$  (Fig. 4b) were produced when iodine was not removed from the reaction. These data indicate the presence of iodine during the formation of magnetite leads to form hematite and maghemite and the formation of hydroxyl groups on the surface of the iron oxide surfaces. Moreover it is noticed that the diffraction data is closer to  $\text{Fe}_3\text{O}_4$  than to  $\gamma\text{-Fe}_2\text{O}_3$ . The present study investigates the types of capping agents on the crystal morphology and size. The diffractograms of magnetite capped with OA, LOA and LNA, Fig.4, displayed six characteristic peaks at  $2\theta = 30.17^\circ, 35.53^\circ, 43.16^\circ, 53.51^\circ, 57.27^\circ,$  and  $62.77^\circ$ , revealing a cubic iron oxide phase ( $\text{Fe}_3\text{O}_4$ , JCPDS No. 89-3854). The broadening of diffraction lines is visible in all samples, indicative of very small crystallites.

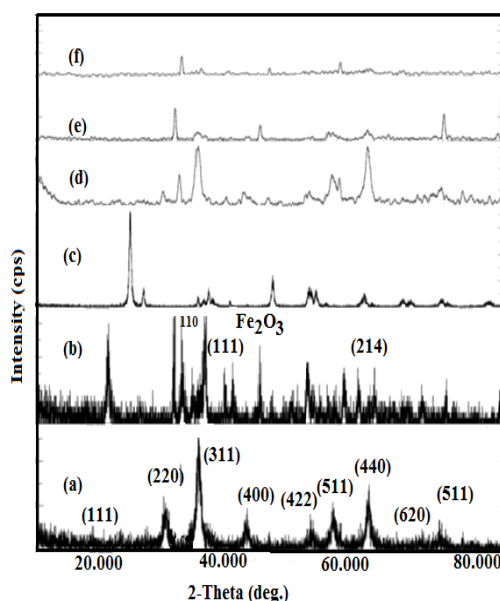


Fig.4: XRD diffractograms of a) magnetite, b) magnetite-iodine, c)  $\text{Fe}_3\text{O}_4/\text{SA}$ , d)  $\text{Fe}_3\text{O}_4/\text{OA}$ , e)  $\text{Fe}_3\text{O}_4/\text{LOA}$  and f)  $\text{Fe}_3\text{O}_4/\text{LNA}$ .

It can be also indicated that  $\text{Fe}_3\text{O}_4$  was coated by OA, LOA and LNA, without destroying the crystal structure. Fig.4c confirms the formation of maghemite beside magnetite although SA was used as capping agent. This means that SA is not able to protect magnetite from oxidation to maghemite. Using the Debye–Scherrer equation diffraction angle ( $2\theta=35.58^\circ$ ) the crystallite size of nanoparticles was estimated.  $D = k\lambda / \beta \cos \theta$ ; where  $k=0.9$  is the Scherrer constant,  $\lambda=0.154\text{nm}$  is the X-ray wavelength,  $\theta$  is the diffraction angle in degrees ( $2\theta= 35.58^\circ$ ) and  $\beta$  is the peak width at half maximum height of the peak [38, 39]. The crystallite sizes of magnetite prepared in the absence and presence of iodine are 10 and 6 nm, respectively. While the crystal size of magnetite coated with SA, OA, LOA and LNA in the presence of iodine are 33.5, 27.3, 20.4 and 14.5 nm, respectively. These data indicates that the crystal sizes decrease with increasing the contents of double bonds when fatty acids are used as capping agents for magnetite.

### 3.3. Morphology and particle size

The shape, dispersability and size of the magnetic nanoparticles are important parameters for their applications. TEM, DLS and zeta potential are effective tools to investigate the magnetite colloid stability. TEM micrographs of magnetite coated with SA, OA, LOA and LNA illustrated in Fig. 5.

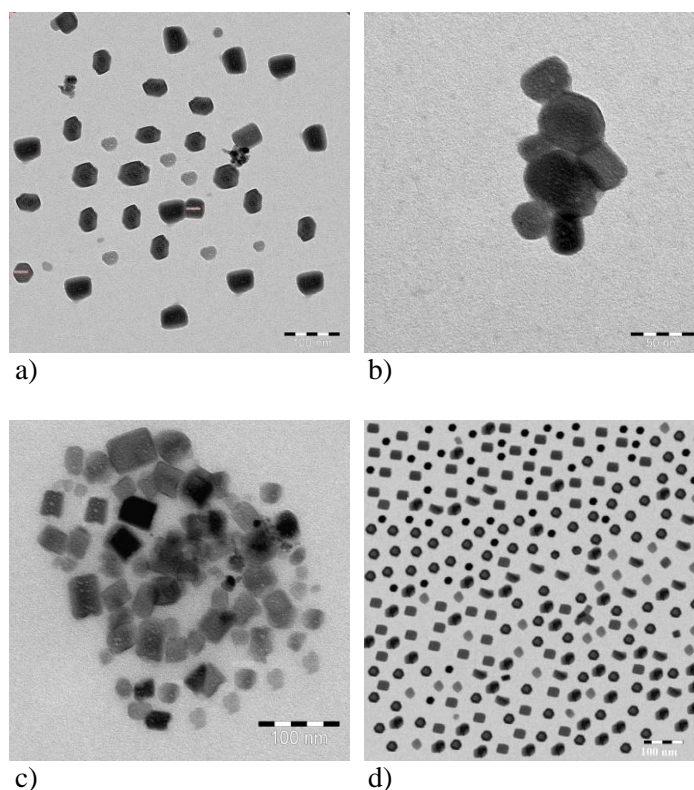


Fig.5: TEM photo of a)  $Fe_3O_4/SA$ , b)  $Fe_3O_4/OA$ , c)  $Fe_3O_4/LOA$  and d)  $Fe_3O_4/LNA$ .

It is clearly observed agglomeration of nanoparticles occur to some extent. Whatever, the colloidal stability of magnetite nanoparticles increases due to successful stabilization of  $Fe_3O_4$  nanoparticles. It is observed that the aggregates decrease with the coating of nanoparticles with fatty acids having more double bonds. This can be referred to the repulsion between  $\pi$  electrons of double bond of fatty acids (OA, LOA and LNA) which prevents full aggregation of nanoparticles. It is also observed that the cubic nanoparticles and nano-rods are highly obtained. The spherical morphology was not observed. Fig.4a shows the TEM micrograph of stearic acid coated  $Fe_3O_4$  nanoparticles. The micrograph show the presence of some aggregations in contrast to the image obtained using unsaturated fatty acids. This behavior mainly attributed to absence of double bond in the hydrocarbon chain of stearic acid. The presence of double bond enhances stabilization of nanoparticles by preventing the aggregation process among the hydrocarbon chains as a result of repulsive forces between  $\pi$  electrons of double bonds. The average particle size obtained from TEM micrograph (Fig. 5) of magnetite coated with SA, OA, LOA and LNA in the presence of iodine are 30.1, 25.3, 20.2 and 15.5 nm, respectively. The particle size dimensions agree with that determined from XRD analysis which indicated the purity of magnetite coated nanoparticles. The OA coated magnetite nanoparticles suffer from some aggregation in aqueous media because it is difficult to make complete dispersion after complete precipitation using organic coating (Fig. 5 b). Also, all nanoparticles have wide size distribution. The differences of the magnetite morphologies from hexagonal, octahedral, cubic to rods were previously referred to the reaction conditions [40, 41]. Moreover, the polyhedral crystals are favored due to extended growth that lead to well-ordered crystallographic (100) and (111) faces. The presence of crystalline planes in the high resolution TEM micrographs of magnetite coated with LNA (Fig. 5 d) confirms the crystalline nature of these MNCs. It is well established that the size distributions and surface charges of the magnetite nanoparticles are behind stability and dispersability of particles in solutions [32]. The aggregates cannot be formed for the particles having higher charge via smaller size due to repulsive forces (scheme 1b). Careful inspection of data indicate that the zeta potential of the magnetic increase from +3.0 mV 46.93 mV when magnetite coated with LNA leading to monodisperse particles with diameter 14.8 nm and polydispersity index (PDI) 0.02. It was

previously reported that, a nanometer system is stable enough when the absolute value of zeta potential is higher than 30 mV [32]. So, the magnetite coated with LOA and LNA have better stability and good dispersibility in ethanol/water (60/40) than that coated with SA and OA. Moreover, the OA, LOA and LNA layers could provide stability against aggregation, which increase the possibility of using magnetite nanoparticles for environmental applications. The colloidal stability, particle size and dispersability of magnetite coated with fatty acids were also investigated by DLS and zeta potential. The data were summarized and listed in Table 1.

Table 1. The DLS and Zeta Potential measurements of the samples.

Sample	DLS		Zeta Potential (mV)
	(nm)	PDI	
Fe <sub>3</sub> O <sub>4</sub> /SA	30.3 ± 11	0.98	10.83 ± 0.60
Fe <sub>3</sub> O <sub>4</sub> /OA	26.9 ± 9.5	0.78	25.53 ± 0.70
Fe <sub>3</sub> O <sub>4</sub> /LOA	20.5 ± 1.0	0.09	37.89 ± 0.65
Fe <sub>3</sub> O <sub>4</sub> /LNA	14.80 ± 0.79	0.02	46.93 ± 0.42

### 3.4. Magnetic and antimicrobial activity

The magnetic properties of nanoparticles are very important parameter for application of magnetic materials in the environments. Moreover, the particle size, shape, nature of the single domain structure of magnetic nanoparticles affect the magnetic properties of nanomaterials [42]. The saturation magnetization ( $M_s$ ) is the state reached when an increase in applied external magnetic field  $H$  cannot increase the magnetization of the material further. The magnetic properties of the magnetite nanoparticles capped with SA, OA, LOA and LNA were studied using a VSM. Fig. 6 shows the magnetization curves of dry magnetite nanoparticles coated with SA, OA, LOA and LNA, respectively at room temperature. It is noticed that,  $M_s$  values of magnetite coated with LNA, LOA, OA and SA are yielding 73, 61, 30 and 15 emu/g, respectively, which are roughly the saturation magnetization of the bulk material ( $M_s^{\text{bulk}} = 82 \text{ Am}^2/\text{kg}$ ) [43]. The high reduction of  $M_s$  of magnetite coated with SA confirms the oxidation of magnetite to maghemite (as observed in the TGA). A great reduction in  $M_s$  value was reported for much smaller magnetic nanoparticles covalently coated with dextran probably due to surface effects [44]. It is well established that the  $M_s$  values increased as particle size increased [45]. The present work is against this rule. These results suggest that the crystal field associated with the new  $\text{O}^{2-}$  surface ligands of the fatty acid coatings that the Fe surface cations suffer resembles that of the Fe bulk cations and helps to reduce the surface spin disorder. These data indicated that the coating of magnetite with LNA and LOA nanocrystals are close to the superparamagnetic limit. Magnetic biomaterials and nanoparticles with size less than 100 nm have the ability to attach with microbial cells. It is very important to investigate the microbial activity, bio-compatibility and toxicity before applications in medical and environment. The present work aims to measure the antibacterial properties of magnetite nanoparticles coated with Sa, OA, LOA and LNA against Escherichia coli (E. coli) and Staphylococcus aureus (S. aureus) as common bacterial strains to determine the minimum inhibition concentration and percent of inhibition of colnier growth. The data of antimicrobial inhibition of magnetite nanoparticles were measured and summarized in Table 2. The data indicate that the magnetite coated with LNA and LOA are highly effective to inhibit bacteria more than that coated with SA and OA at minimum inhibition concentration (MIC;  $\text{mg mL}^{-1}$ ) as listed in Table 2.

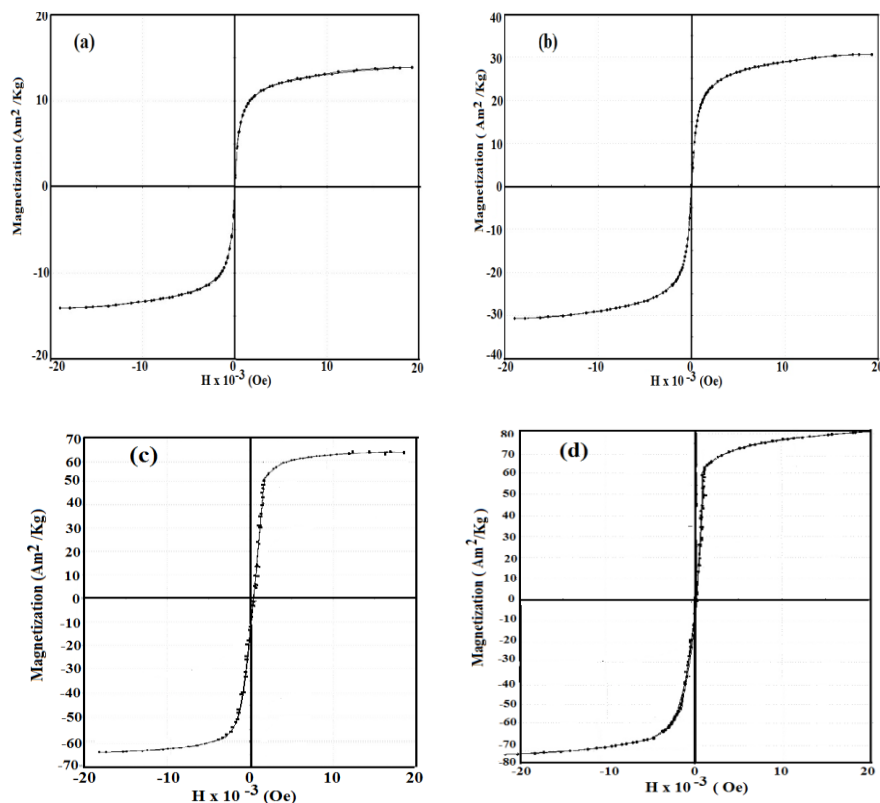


Fig.6: VSM of a)  $Fe_3O_4/SA$ , b)  $Fe_3O_4/OA$ , c)  $Fe_3O_4/LOA$  and d)  $Fe_3O_4/LNA$ .

Table 2. MIC (minimum inhibition concentration) values ( $mg\ mL^{-1}$ ) of sample against *Escherichia coli* ATCC 8739, *Staphylococcus aureus* ATCC 6538 strains.

Antimicrobial materials		MIC ( $mg\ mL^{-1}$ )	The percent (%) inhibition of colonier growth
$Fe_3O_4$	<i>E. coli</i>	10	31±9
	<i>S. aureus</i>	1	48±4
$Fe_3O_4/SA$	<i>E. coli</i>	1	36±9
	<i>S. aureus</i>	2.5	33±4
$Fe_3O_4/OA$	<i>E. coli</i>	1	40±12
	<i>S. aureus</i>	0.25	34±11
$Fe_3O_4/LOA$	<i>E. coli</i>	2.5	55±4
	<i>S. aureus</i>	5	75±7
$Fe_3O_4/LNA$	<i>E. coli</i>	1	84±6
	<i>S. aureus</i>	2.5	79±4

Careful inspection of data confirms that the prepared materials have exceptional antimicrobial activity which was attributed to their higher surface area to volume ratio of the

MNPs coated with LNA and LOA as determined from DLS and TEM analyses and hence the greater available surface of the antibiotic that was in contact with the microorganisms. Lee et al. [46] reported that the inactivation of *E. coli* by zero-valent iron nanoparticles may be attributed to the penetration of the small particles (sizes ranging from 10 to 80 nm) into *E. coli* membranes, leading to oxidative stress and causes disruption of the cell membrane. These data indicated that the magnetite coated with fatty acids had a positive effect on the antimicrobial activity. The presence of OH, COOH and COO groups and magnetite content played significant roles in the bactericidal efficacy and mechanism [47]. Fatty acids are known to have antibacterial and antifungal properties [48]. Thus, such magnetite coated nanoparticles with SA, OA, LOA and LNA can be used for oil spill collector without being cytotoxic. Moreover, due to the unique characteristics of synthesized  $\text{Fe}_3\text{O}_4$  coated with SA, OA, LOA and LNA thin films represent a competitive candidate for the development of novel biomedical surfaces or devices with low costs and a high efficiency.

### 3.5. Evaluation of magnetite as oil spill collector

Oil spills have devastating energy and environmental consequences in the last decades. There are several fast techniques used to alleviate the pollution such as boom and oleophilic surface skimmers, dispersants and oil sorbers. The efficiency of oil recovery of such technology does not exceed 50% depending on factors such as the type and thickness of oil, presence of waves, etc [49]. The basic premise of this work was to collect oil spills after spreading the prepared magnetic powder over oil surfaces followed by separation using magnetic forces. There are several requirements should be included to apply this method which materials used should be reusable and environmentally safe and use none/very little energy [50]. The goal is to have the ferromagnetic particles that spread and mix with the spilled oil, making it magnetic without losses of materials in water. The oil can be removed from the water using a neodymium magnet. The goal is also seek to quantify how efficient is the method in removing oil from water. Moreover, recovering the magnetic component of the magnetic phase for reuse and repeating the process to obtain sufficient separation to discard the water phase while storing the oil phase for transport to a refinery facility. The data of oil recovery efficiency determined via variation of magnetite oil ratio (MOR) were measured and summarized in Table 3. The data confirm that the magnetite coated with LNA and LOA possess good oil collection at MOR 1:25 which correlated to their higher saturation magnetization than magnetite capped with OA and SA. Moreover, although uncoated magnetite has strong magnetic saturation, it achieved low oil spill collector (Table 3) due to low hydrophobicity of uncoated magnetite. The data of reuse of magnetite capped materials indicated that the ability to recovery 80 % of used magnetite and reused 3 times with the same efficiency.

Table (3): Oil collection efficiency of magnetite and fatty acids capped magnetite nanoparticles.

Magnetite	Efficiency of oil removal at different MOR			
	1:1	1:5	1:10	1:25
$\text{Fe}_3\text{O}_4$	45	20	10	5
$\text{Fe}_3\text{O}_4/\text{SA}$	80	75	67	50
$\text{Fe}_3\text{O}_4/\text{OA}$	88	80	72	65
$\text{Fe}_3\text{O}_4/\text{LOA}$	100	97	95	90
$\text{Fe}_3\text{O}_4/\text{LNA}$	100	99	97	95

## 4. Conclusions

Magnetite nanoparticles capped with SA, OA, LOA and LNA were prepared on the large scale using new method at low temperature. Capping of magnetite with fatty acid were carried out insitue during preparation process of of magnetite nanoparticle. The quantity of acids used for magnetite capping determined from surface tension measurements. Formation of hydroxyl groups

on the surface of iron oxide nanoparticles enhance the capping of the particles with fatty acid and these groups are able to form covalent bonds with carboxylic functional groups of fatty acids to avoid their agglomeration. The ester was not formed between SA and magnetite can be attributed to the attraction between alkyl groups of SA at magnetite surface will hinder the chemisorption at magnetite surfaces. XRD data indicated the formation of maghemite beside magnetite when the magnetite nanoparticles coated with SA. TEM data indicated for the first time the formation of magnetite nano-cubes and nano-rods without usual formation of nanosphere coated magnetite in the coprecipitation method. The high magnetism, stability against aggregation, and high antimicrobial efficiencies of magnetite nanoparticles capped with LNA and LOA drives toward using magnetite nanoparticles as oil spill collectors.

### Acknowledgments

This project was supported by King Saud University, Deanship of Scientific Research, and Research Chair.

### References

- [1] M. Mahmoudi, S. Sant, B. Wang, S. Laurent, Sen T. *Adv Drug Deliv Rev.* **63**, 24–46 (2011).
- [2] J.M. Rosenholm, J. Zhang, W. Sun, H. Gu, *Microporous and Mesoporous Mater.* **145**, 14-20 (2011).
- [3] N. Ye, Y. Xie, P. Shi, T. Gao, J. Ma, *Mate. Sci. Eng.: C* **45**, 8-14 (2014).
- [4] Xiong Y, Ye J, Gu X, Chen Q, *J. Magn.Magn. Mater.* **320**, 107–112 (2008).
- [5] F. Furno, K.S. Morley, B. Wong, *J. Antimicro. Chem.* **54**, 1019–24 (2004).
- [6] R.K. Singh, T.H. Kim, K.D. Patel, J.C. Knowles, H.W. Kim, *J. Biomed. Mater. Res A* **100**, 1734–42 (2012).
- [7] A.M. Grumezescu, *Curr Org Chem* **17**, 90–96 (2013).
- [8] I. Liakos, A.M. Grumezescu, A. M. Holban, *Molecules* **19**, 12710-26 (2014).
- [9] A. Figuerola, R. di Corato, L. Manna, T. Pellegrino, *Pharmacol. Res.* **62**, 126–143 (2010).
- [10] M.C. Chifiriuc, A.M. Grumezescu, C. Saviuc, R. Hristu, V. Grumezescu, C. Bleotu, G. Stanciu, D.E. Mihaiescu, E. Andronescu, V. Lazar, *Curr. Org. Chem.* **17**, 1023–28 (2013).
- [11] M.C. Chifiriuc, V. Lazar, C. Bleotu, I. Calugarescu, A.M. Grumezescu, D.E. Mihaiescu, D.E. Mogoşanu, A.S. Buteica, E. Buteica, *Digest. J. Nanomater. Biostruct.* **6**, 37-44 (2011).
- [12] J.A. Lopez, F. González, F.A. Bonilla, G. Zambrano, M.E. Gómez, *Rev Latin Am Metal Mat* **30**, 60-66 (2010).
- [13] S. Sun, H. Zeng, *J. Amer. Chem. Soc.* **124**, 8204-05 (2002).
- [14] S.Arokiyaraj, M. Saravanan, N.K. Prakash, M.V. Arasu, B. Vijayakumar, S. Vincent, *Mater. Res.earch Bull.* **48**, 3323–27 (2013).
- [15] W.Y. Chen, L. Ju-Yu, C. Wei-Jen, L. Liyang, E.W. Guang Diao, Y.C. Chen, *Nanomedicine* **5**, 755–764 (2010).
- [16] P. Antoniea, C. Dorina, N. Claudia, T.F. Mihai, *Afr. J. Microbiol. Res* **6**, 1054– 60 (2012).
- [17] B.S. Inbaraj, T.Y. Tsai, B.H. Chen, *Sci Technol Adv Mater.* **13**, 015002 (2012).
- [18] D.E. Mihaiescu, A.M. Grumezescu, A.S. Rumezescu, D.E. Buteica, P.C. Mogosanu, O.M. Balaure, *Dig. J. Nanomater. Biostruct.* **7**, 253–60 (2012).
- [19] T. Togashi, M. Umetsu, T. Naka, S. Ohara, Y. Hatakeyama, T. Adschiri, *J.Nanoparticle Res.* **13**, 3991–99(2011).
- [20] M.M. Rashad, H.M. El-Sayed, M. Rasly, M.I. Nasr, *J. Magn. Magn. Mater.* **324**, 4019–23 (2012).
- [21] G.H. Gao, X.H. Liu, R.R. Shi, K.C. Zhou, Y.G. Shi, R.Z. Ma, T.E. Takayama, G.Z. Qiu, *Crystal Growth and Design* **10**, 2888–28 (2010).
- [22] G.H. Gao, R.R. Shi, W.Q. Qin, Y.G. Shi, G.F. Xu, G.Z. Qiu, X.H. Liu, *J. Mater. Sci.* **45**, 3483–89 (2010).
- [23] M. Abbas, M. Takahashi, C. Kim, *J.Nanoparticle Res.* **15**, 1365 (2013).

- [24] Y.F. Zhu, W.R. Zhao, H.R. Chen, J.L. Shi, *Journal of Physical Chemistry C* **111**, 5281–85 (2007).
- [25] X. Zhou, Y.F. Shi, L. Ren, S.X. Bao, Y. Han, S.C. Wu, H.G. Zhang, L.B. Zhong, Q.Q. Zhang, *J. Solid State Chem.* **196**, 138–144 (2012).
- [26] Y.Y. Zheng, X.B. Wang, L. Shang, C.R. Li, C. Cui, W.J. Dong, W.H. Tang, B.Y. Chen, *Mater. Charact.* **61**, 489–92 (2010).
- [27] A.M. Atta, G.A. El-Mahdy, H.A. Al-Lohedan, S.A. Al-Hussain, *Int. J. Mol. Sci.* **15**, 6974–89 (2014).
- [28] R. Massart, *IEEE Transactions* **17**, 1247–48 (1981).
- [29] G.A. El-Mahdy, A.M. Atta, H.A. Al-Lohedan, *J. Taiw. Inst. Chem. Eng.* **45**, 1947–53 (2014).
- [30] G.A. El-Mahdy, A.M. Atta, H.A. Al-Lohedan, *Molecules* **19**, 1713–31 (2014).
- [31] A.M. Atta, A.K.F. Dyab, Coated Magnetite Nanoparticles, Method for the Preparation thereof and Their Use. EP 13167616.5, (2013).
- [32] A.M. Atta, H.A. Al-Lohedan, S.A. Al-Hussain, *Molecules* **19**, 11263–78 (2014).
- [33] M.I. Khalil, Process for Preparing Magnetic (Fe<sub>3</sub>O<sub>4</sub>) and Derivatives thereof. EP 2505558 A1, 2013.
- [34] T. Nagata, K. Fukushi, *Geochim. Cosmochim. Acta* **74**, 6000–13 (2010).
- [35] S. Yokoyama, M. Nakagaki, *Colloid Polym. Sci.* **271**, 512–18 (1993).
- [36] D. Ortega, Q.A. Pankhurst, *Nanoscience* **1**, 60–88 (2013).
- [37] S. Sharifi, S. Behzadi, S. Laurent, M.L. Forrest, P. Stroeve, M. Mahmoudi, *Chem. Soc. Rev.* **41**, 2323–43 (2012).
- [38] W. Kim, C-Y. Suh, S-W. Cho, K-M. Roh, H. Kwon, K. Song, *Talanta* **94**, 348–52 (2012).
- [39] H.P. Klug, L.E. Alexander, *X-ray Diffraction Procedures for Polycrystalline and Amorphous Materials*, John Wiley & Sons, New York, p. 491 (1962).
- [40] G. Salas, C. Casado, F.J. Teran, R. Miranda, C.J. Serna, M.P. Morales, *J. Mater. Chem.* **22**, 21065–75 (2012).
- [41] R.M. Cornell and U. Schwertmann, in *The Iron Oxides: Structure, Properties, Reactions, Occurrences and Uses*, ed. Wiley VCH, 2nd ed., ch., pp128. 21(2003).
- [42] R. H. Kodama, *J. Magn. Magn. Mater.* **200**, 359–372 (1999).
- [43] K. O’Grady, A. Bradbury, *J. Magn. Magn. Mater.* **39**, 91–94 (1983).
- [44] M. Creixell, A.P. Herrera, M. Latorre-Esteves, V. Ayala, M. Torres-Lugo, C. Rinaldi, *J. Mater. Chem* **20**, 8539–47(2010).
- [45] B.D. Cullity and C.D. Graham, in *Introduction to Magnetic Materials*, ed. Wiley, 2nd edn., (2009).
- [46] C. Lee, J.Y. Kim, W.I. Lee, K.L. Nelson, J. Yoon, D.L. Sedlak, *Environ. Technol* **42**, 4927–33 (2008).
- [47] S.L. Iconaru, A.M. Prodan, M. Motelica-Heino, S. Sizaret, D. Predoi, *Nanoscale Res. Lett.* **7**, 576–83(2012).
- [48] L.J. McGaw, A.K. Jäger, J. Van Staden, *Fitoter.*, **73**, 431–433 (2002).
- [49] M. Fingas, *Oil Spill Science and Technology*: Elsevier, (2011).
- [50] M. Zahn, Magnetic Colloid Petroleum Oil Spill Clean-up of Ocean Surface, Depth and Shore Regions," USA Patent Application No. #13/369,338 (2011).